Calculation of the Internal Blast Pressures for Tunnel Magazine Tests

by

Kevin Hager
Naval Facilities Engineering Service Center
Pt Hueneme, CA

and

Naury Birnbaum
Century Dynamics, Inc.
San Ramon, CA

ABSTRACT

An underground storage facility can be very complicated. It may include multiple storage chambers, access tunnels, and exits. Prediction of the internal and external pressure environment, for developing explosives safety criteria, has been done with limited success.

The Naval Facilities Engineering Service Center was tasked by the Department of Defense Explosives Safety Board to predict the internal blast environment for specific tunnel magazine tests. The dynamic pressure environment was calculated using AUTODYN-2D and -3D. Effects of tunnel geometry and media surrounding the tunnel on the load environment are presented and compared to test data.

1.0 Introduction.

Criteria for the safe siting of inhabited buildings near underground ammunition storage facilities are found in Department of Defense (DOD) Directive 6055.9. Each service within the DOD has additional criteria applicable for service unique weapons and associated safety requirements. Safety criteria common to all underground storage tunnels define Inhabited Building Distances (IBD) to prevent loss of life and property from debris throw, shock pressures, and ground shock.

The design of underground storage facilities may include several separate chambers for storing ammunition, secondary tunnels for connecting the chambers, and primary tunnels for entering and exiting the facility. Methods for reducing IBD include blast traps and closure devices to reduce shock pressures traveling through secondary and primary tunnels to the facility exit. In all cases, tunnel designs for mitigating shock

Report Documentation Page

Form Approved
OMB No. 0704-0188

1. REPORT DATE	2. REPORT TYPE	3. DATES COVERED
AUG 1996		**00-00-1996 to 00-00-1996**

4. TITLE AND SUBTITLE	5a. CONTRACT NUMBER
Calculation of the Internal Blast Pressures for Tunnel Magazine Tests	5b. GRANT NUMBER
	5c. PROGRAM ELEMENT NUMBER
6. AUTHOR(S)	5d. PROJECT NUMBER
	5e. TASK NUMBER
	5f. WORK UNIT NUMBER
7. PERFORMING ORGANIZATION NAME(S) AND ADDRESS(ES) **Naval Facilities Engineering Service Center, ,1100 23rd Avenue,Port Hueneme,CA,93043**	8. PERFORMING ORGANIZATION REPORT NUMBER
9. SPONSORING/MONITORING AGENCY NAME(S) AND ADDRESS(ES)	10. SPONSOR/MONITOR'S ACRONYM(S)
	11. SPONSOR/MONITOR'S REPORT NUMBER(S)

12. DISTRIBUTION/AVAILABILITY STATEMENT
Approved for public release; distribution unlimited

13. SUPPLEMENTARY NOTES
See also ADM000767. Proceedings of the Twenty-Seventh DoD Explosives Safety Seminar Held in Las Vegas, NV on 22-26 August 1996.

14. ABSTRACT
see report

15. SUBJECT TERMS

16. SECURITY CLASSIFICATION OF:			17. LIMITATION OF ABSTRACT	18. NUMBER OF PAGES	19a. NAME OF RESPONSIBLE PERSON
a. REPORT **unclassified**	b. ABSTRACT **unclassified**	c. THIS PAGE **unclassified**	**Same as Report (SAR)**	**22**	

pressures are site specific and require test and analysis to prove the effectiveness of the design.

Testing to prove the effectiveness of closure devices and blast traps has required a series of small scale development tests followed by full scale certification tests. Such tests are expensive, typically site specific, and limit the number of feasible designs to be tested. Validation of analytical procedures may reduce the cost of testing, and permit generic designs to be applied to multiple sites.

1.1 Objective. The objective of this effort is to:

(a) predict the pressure environment for a storage chamber, a secondary tunnel , and a primary tunnel inside an underground storage facility,

(b) determine the effects of tunnel length, and responding and nonresponding boundary conditions on peak shock pressures and time duration of pressures, and

(c) compare measured and predicted pressure time-histories.

1.2 Scope. The U.S. Army Engineer Waterways Experiment Station (WES) has completed a series of tests to measure the effectiveness of various tunnel designs. The Naval Facilities Engineering Service Center (NFESC) has been tasked by the DOD Explosive Safety Board (DDESB) to analyze an underground explosive test and compare measured and predicted results. This task supports the DDESB effort for evaluating analytical procedures to predict pressure environments inside and outside of underground storage facilities.

This document will report on measured and predicted shock pressures for an underground explosives test. Analysis of debris throw and ground shock is outside of the scope for this report. The analysis will consist of the following three sections:

(a) The peak pressures at different locations inside straight tunnels will be calculated. The effect of tunnel length on attentuating peak pressures will be shown.

(b) The peak pressures at different locations within a tunnel complex will be calculated. The effects of tunnel length and multiple junctions on peak pressures will be calculated with a two-dimensional, planar model.

(c) The peak pressures at different locations within a tunnel complex will be calculated. The effects of tunnel length and multiple junctions will be calculated with a three-dimensional model.

In each of the first two cases, the effects of nonresponding and responding media will be shown. In the third case, only the effects of responding media along the tunnel surfaces will be analyzed.

2.0 Explosive Testing: Setup and Measured Results

The tunnel complex is designed to evaluate methods of mitigating pressures exiting storage chambers from an accidental explosion. Pressure load and ground shock motion have been measured for several tests conducted in different storage chambers. This section presents the general layout of the tunnels and storage chambers, locations of pressure gages, and measured pressure loads for one explosive test.

2.1 Tunnel Layout. The tunnel complex consists of a main tunnel with two side drift tunnels. As shown in Figure 1, the junction of the main tunnel and the left drift tunnel is located 250 m from the entrance of the main tunnel. The main tunnel extends 25m beyond this junction.

Four test chambers are located along the 98 m length of the left drift tunnel. All of the storage chambers are 8m long by 4m wide by 2m high. Each storage chamber is connected by a single, access tunnel to the left drift tunnel. Unlike the storage chambers, each access tunnel has a unique geometry to test the effects of length and shape on pressures measured at gage locations in the tunnel complex.

The pressure data presented in this section is based on an explosive test conducted in Chamber #4. The charge is 2826 kg of Comp B explosive. The charge weight to volume for the chamber is 44.1 kg/m^3. The access tunnel is a straight tunnel and has a 1.5m wide by 1.5m high cross-section.

2.2 Pressure Gage Locations. Figure 2 shows the location of the pressure gages along the length of the left drift tunnel. Gages measuring side-on pressures are located along the center-line of the tunnel in front of each access tunnel.

2.3 Measured Pressure Time Histories.

Table 1 lists the peak side-on pressures recorded at gages located between the donor chamber (Chamber No. 4) and the main tunnel exit. Column two of the table shows the range from the center of the donor to the pressure gage. The measured peak side-on pressure decreases with increasing distance from the charge. The measured peak pressure from Table 1 are plotted in Figure 3.

Figures 4 and 5 show the measured pressure time-histories for gages 26 and 10. Gage 26 is located in the Left Drift tunnel in front of the access tunnel to Chamber No. 4. Gage 10 is near the junction of the drift and main tunnels. Gage 26 measures a shock phase of less than 500 ms duration followed by quasi-static pressure of 2500 kPa. This quasi-static pressure remains constant until the end of the time record. Gage 10 measures an initial shock phase which decays rapidly. After the initial shock phase, the pressure

buildups over 700 ms to a peak pressure of 1049 kPa. The measured pressure requires at least 9 seconds to exponentially decays from the peak pressure back to ambient pressure.

3.0 Numerical Analysis.

This section documents the model setup and predicted load environment at different locations inside the tunnel complex. Analysis of the load environment has been completed using AUTODYN-2D, a commercial software programs from Century Dynamics, San Ramon, CA.

AUTODYN-2D uses finite difference algorithms to calculate the detonation and expansion of explosives, and the propagation of shock waves though solids and gases. Solids, such as limestone and granite, are modeled with Lagrange based meshes which deform and move with the material. Gases, such as air and explosive by products, are modeled with Euler based meshes which remain stationary. Material undergoing large strains and displacements are transported from cell to cell in an Euler mesh. For the tunnel calculations with responding media, the rock is modeled with Lagrange meshes and all gases are modeled with Euler meshes. Overlapping Euler and Lagrange meshes interact with each other across interface elements. At the interface, the Lagrange mesh constrains material movement among euler mesh cells and the Euler mesh applies pressure loads against the Lagrange mesh surface.

3.1 Straight Tunnels. This section reports the analytical predictions of internal and external pressures of straight axisymmetric tunnels. Three calculations of the load environment inside the chamber, the access tunnel and outside the tunnel exit have been completed. The goal of these calculations is to show the effect of access tunnel length and responding surrounding the tunnel on predicted pressure loads.

A conceptual, AUTODYN-2D model of the chamber, the access tunnel, and open atmosphere is shown in Figure 6. The chamber, access tunnel, open atmosphere are modeled as three cylinders attached end to end. All three cylinders are located along the same center-line axis. The chamber is 8 meters long by 3.19 meters in diameter. A 2826 kg spherical charge is located at the center of the chamber. The ratio of charge weight to chamber volume is 44.2 kg/m^3. Depending on the model, the length of access tunnel varies from 100 meters to 200 meters. The radius of the access tunnel is 1.14 meters along the length of the tunnel. The cylinder representing the open atmosphere is 50 meters in diameter and 210 meters long.

In the AUTODYN-2D, the cylinders are constructed from axisymmetric, eulerian meshes. The axis of rotation is located along the center-line axis of the three cylinders. Eulerian meshes track the detonation and expansion of explosive material and movement of the shock wave.

Two boundary conditions are applied to the surfaces of the cylinders. The perfectly reflecting boundary prevents transmission of shock waves and material through the surface. The surfaces of the chamber and the access tunnel are perfectly reflective surfaces. The flow boundary permits the transmission of shock waves and material through the surface. The flow boundary ideally represents ambient pressure and energy at distances far from the access tunnel exit. The circumference of the open atmosphere cylinder and the surface opposite the access tunnel exit have flow boundaries. The surface attached to the access tunnel is a perfectly reflective surface.

The ranges of the target locations inside the tunnel are listed in Table 2. The ranges shown in column 2 measure the distance from the chamber exit to the target location**.**

Figure7 shows a conceptual, AUTODYN-2D model of the straight tunnel with responding media around the chamber and the access tunnel. The chamber and access tunnel, and open atmosphere are represented by cylinders with the same dimensions used in the model with nonresponding surfaces. The responding media is modeled by a fourth cylinder in which the chamber and access tunnel are embedded. This cylinder representing the responding is 7.8 m in radius and 115 m in length.

The cylinders representing the chamber, access tunnel, and open atmosphere are constructed from axisymmetric, eulerian meshes. The responding media is modeled with an axisymmetric, Lagrange mesh. The axis of rotation is located along the center-line axis of the four cylinders.

Table 2 shows the calculated pressure at different locations in several straight tunnels. Calculated pressures are shown for three tunnels, including:

(a) a 100 m straight tunnel with perfectly reflecting, nonresponding walls,

(b) a 300 m straight tunnel with perfectly reflecting, nonresponding walls, and

(c) a 100 m straight tunnel with a responding media surrounding the tunnel.

Pressure time-histories are calculated at the same points for all three tunnels. These points are located at the range from the donor charge as the pressure gages used in the tunnel complex.

The peak pressures target points 1 through 6 are the same 100 m and 300 m tunnels with nonresponding walls. Peak pressures for the 100m tunnels with and without responding media are similar. The responding media appears to have minimal effect on the peak pressures.

3.2 Two-Dimensional Analysis of the Left Drift and Main Tunnel. This section reports the analytical predictions of internal pressures for the complex of chambers and tunnels described in Section 2.0. Two calculations of the load environment inside the Test Chamber #4, the left drift tunnel and the main access tunnel have been completed. The goal of these calculations is to show the effect of responding and nonresponding media the tunnels on predicted pressure loads.

A typical AUTODYN-2D model of the chambers, the Left Drift Tunnel tunnels, and the junction of the Drift and Main tunnels is shown in Figure 8. The chambers, tunnels, open atmosphere are modeled as interconnected, rectangular planar regions. The regions are constructed from planar, eulerian meshes.

Four test chambers are located along the length of the left drift tunnel. In all planar models of the tunnel complex, a unit height is assumed for all tunnels and chambers. All of the models of the storage chambers are 8m by 8m. The dimensions for the model chambers are chosen to match the 64 m^3 volume of the actual chambers.

The lengths of the drift and main tunnels, and the chamber locations along the drift tunnel in the model are similar to lengths of the actual tunnel complex, see Figure 1. The complex geometry of the different access tunnels are ignored. The access tunnels connecting the chambers to the drift tunnel are modeled as straight short tunnels. In determining the width of the model tunnels, the hydraulic diameter is the model and actual tunnels are assumed to be the same. The hydraulic diameter is defined as the cross-sectional area of the tunnel divided by the cross-sectional perimeter.

Figure 8 shows the target locations for determining pressure time-histories along the length of the left drift tunnel and in the main tunnel. The ranges of the target locations inside the tunnel are listed in Table 3. The ranges shown in column 2 measure the distance from the center of the explosive charge to the target location.

Two boundary conditions are applied along the edges of the planar meshes. The edges for all of the tunnels and chambers have a perfectly reflecting boundaries. The flow boundaries representing ambient pressure and energy are applied to the edges of the mesh modeling the open atmosphere at the tunnel exit.

Figure 9 shows the AUTODYN-2D model of the tunnel complex with responding media surrounding Chamber No. 4, along the edges of the drift tunnel, and around the junction of the drift and main tunnels. The chambers, tunnels, and open atmosphere are represented by euler meshes with the same dimensions used in the model with nonresponding surfaces.

3.3 Three-Dimensional Analysis of the Left Drift and Main Tunnel. AUTODYN-3D was applied to the simulation of the explosion in the tunnel complex. A three dimensional model can avoid the scaling and geometric assumptions required for a two-dimensional analysis. Specifically, the charge size, chamber and tunnel dimensions can

conform more directly with the actual test configuration. An AUTODYN-3D model was constructed including the four chambers, left drift, and part of the main tunnel. To assess the influence of the surrounding media, granite material was included around Chamber #4, where the charge is located, as well as most of the left drift including access tunnels to Chambers #1 and #2. The model is shown in Figure 10.

In the AUTODYN-2D analyses of the straight tunnels and the tunnel complex, Lagrange and Euler meshes were applied selectively to the responding rock media and the tunnels. The euler mesh calculates the detonation of the explosive, expansion of the detonation products, and air flow in the tunnel. The Lagrange mesh simulates the response of the surrounding geologic medium. The two meshes a coupled by a special interface.

However, in the 3D model, a single ALE (Arbitrary Lagrange Euler) mesh is used which allows the gas dynamics contained in the tunnels and chambers to be modeled in Euler while the surrounding rock media is modeled in Lagrange. In the Euler formulation the numerical mesh remains fixed in space with material flowing through it. Thus, Euler is well suited to the gas dynamic flow portion of the problem. In the Lagrange formulation, the numerical mesh is moved and distorted with the material motion. Thus, Lagrange is well suited to modeling the surrounding solid media. The ALE mesh in AUTODYN allows for arbitrary general motions of the numerical mesh between the Euler (fixed) and Lagrange (moving) specifications thereby providing an automatic mesh rezoning capability. In the 3D tunnel blast simulation only strict Lagrange or Euler motions are specified.

The air in the tunnel is initialized to ambient conditions of 100 kPa. The initial detonation and expansion of the 2826 kg charge of COMP B is computed in a finely zoned AUTODYN one-dimensional(1D) spherical symmetric model. The remap facility of AUTODYN is then used to map the initial 1D spherical explosion into the center of the three dimensional chamber #4. The 1D to 3D remapping technique allows for a much more accurate modeling of the initial detonation process than would be allowed by modeling it in the coarser 3D mesh. The cutaway view, shown in Figure 11, exposes the initial explosion region within chamber 4.

The surrounding rock mass boundaries are specified with a transmit boundary condition to allow the shock wave to be transmitted out of the grid simulating the larger surrounding geologic volume. At the ends of the main tunnel, a transmit boundary was also specified to allow the flow to continue out of the grid simulating the much greater length of the tunnel.

The 3D solution was carried out to a time of 300 milliseconds at which time the blast wave has had ample time to exit Chamber #4, traverse the left drift, and enter the main tunnel. Pressure records were taken at a number of locations as shown in Figure 12.

4.0 Comparison of Test Measurements and Analysis

This section reports the compares the measured and predicted of internal pressures for the complex of chambers and tunnels described in Sections 2.0, 3.2, and 3.3. All of the pressures time-histories inside the tunnel complex can be separated into the initial shock phase and the quasi-static gas pressure phase. The initial shock phase accounts for the initial incident and all reflected pressures caused by the shock wave traveling from the donor chamber to the tunnel exit. The quasi-static phase accounts for the buildup gas pressures inside the tunnel complex, and for the venting of gases from the tunnel exit.

Figures 13 and 14 compare the predicted and measured pressure time-histories at Gages 10 and 26. Note, the predicted pressures are based on the Autodyn-2D models. Gage 10 is located near the junction of the Left Drift and Main Tunnels. Gage 26 is located in the Left Drift Tunnel in front of the access tunnel for Chamber No. 4. The measured shock phases for both locations are completed in less than 500 msec after detonation of the donor. Duration of the predicted shock phases is approximately 2000 msec for both locations. Table 3 shows that the predicted from the peak pressures (from the Autodyn two-dimensional models) are significantly higher than the measured pressures. For example, Autodyn-2D predicts peak pressures at Gage 26 in excess of 24,000 kPa. The measured pressure is 13,103 kPa. At Gage 10, Autodyn-2D predicted peak pressures a factor of ten larger than the measured pressure.

The measured quasi-static pressures, shown in Figures 13 and 14, last up to ten seconds after detonation. At Gage 26, this pressure remains constant at 2500 kPa, while the predicted pressure decays to less than 1000 kPa. At Gage 10, the quasi-static pressure reaches a peak of 1050 kPa and then decays to back to atmospheric pressure. The predicted quasi-static pressures at Gages 26 and 10 are similar. The measured quasi-static pressures at these gages show the most significant differences.

Figure 15 shows the emergence and separation of the shock wave from the tunnel exit. The shock wave exits the tunnel complex in less than 184 msec after detonation of the explosive charge. Separation of the shock wave from the tunnel is completed by 220 msec after detonation. The quasi-static pressures inside the tunnel complex no longer affect the external pressures at large distance from the tunnel exit. The venting of the quasi-static pressures at the tunnel exit simulates a high velocity, energetic gas jet entering a large volume with low energy, low density gas. The pressure environment caused by this venting is localized to the tunnel exit.

Figure 16 shows the pressure time-histories predicted by Autodyn-3D. This figure shows attenuation of the peak pressures as the shock wave travels down the Left Drift tunnel. Note that a sharp, initial peak pressure is resolved only for Gage 26. The pressures time-histories at all other gages show a buildup to a constant pressure. The pressures predicted by Autodyn-3D exceed the measured peak pressures by a factor of five at Gages 17 and 25. The difference in predicted and measured peak pressure at Gage 26 is less than 20%.

Figure 17 plots the measured peak pressures, and the predicted pressures from the Autodyn-2D and -3D models. Both the Autodyn-3D and the measured peak pressures show a reduction in peak pressures with increasing distance from the donor charge. Autodyn-2D shows a reduction follow by an increase in the peak pressures. Reflected pressures from the tunnel junction be causing the higher pressures for gages close to the junction.

5.0 Conclusions

Several calculations have been completed to show the effects of tunnel geometry and responding media on peak pressures inside a underground ammunition storage complex. The conclusions are summarized in the following:

(a) For straight tunnels, the peak pressures attenuated slowly along the length of the tunnel. Responding media along the tunnel walls caused minimal change in the predicted peak pressures.

(b) For the tunnel complex, responding media reduced peak pressures near Chamber No. 4 and along the Left Drift by 10 to 30%.

(c) Predicted peak pressures exceed the measured pressures by at least 100% near Chamber No. 4. At the junction to the Left Drift and Main Tunnels, Autodyn-2D predicts pressures ten times higher than the measured pressure. These overpredicted pressures may be the resulted of overpredicted reflected pressures at the tunnel junction.

(d) Autodyn-2D predicted long term quasi-static pressures which agreed well with the measured duration of the pressures. Accurate prediction of the magnitude of the pressures is still uncertain. The magnitude of the measured quasi-static pressures vary significantly among pressure gages. Also, the effect of boundary conditions for the open atmosphere on the quasi-static pressure is not resolved.

(e) Accurate prediction of external pressures at large distances from the tunnel exit will depend on accurate prediction of internal peak pressures. Because of the separation of the shock wave from the tunnel exit, the long duration quasi-static pressures will have little impact on IBD outside the tunnel.

6.0 Recommendations

Recommendations for future work includes:

(a) Calculate the internal pressure environment for straight tunnels using other software, including CTH. The goal is to identify if material models and boundary conditions available in CTH may yield better pressure prediction. CTH has a library of materials

which will enable a parameter study of the effects of material models on internal tunnel pressure.

(b) Complete Autodyn-3D calculations with finer meshing to determine if the observed pressure attenuation is caused by mesh size or by “numerical” effects of using ALE meshing of the tunnel complex.

Table 1. Internal Load Environment, Measured Peak Side-on Pressures

Pressure Gage	Range[1]	Location	Peak Pressure (kPa)
26	10.25	Left Test Drift	13103
25	19.09	Left Test Drift	2898
17	27.18	Left Test Drift	6750
16	37.95	Left Test Drift	1660
10	73.64	Left Test Drift	1049
1	320.01	Main Tunnel	66.22

[1] Distance is measured from center of explosive charge.

Table 2. Comparison of Calculated Straight Tunnel Pressures and Measured Side-on Pressures

Range	Tunnels without Responding Media		Tunnels with Responding Media	Measured Peak Pressures
	100 m Tunnel	300 m Tunnel	100 m Tunnel	Tunnel Complex
(m)	(kPa)	(kPa)	(kPa)	(kPa)
10.2	28190	28190	30610	13100
19.0	16590	16090	16820	2880
27.0	14500	14500	16150	6750
37.8	13540	13540	12410	1660
49.8	11300	11300	10730	
73.4	9530	9530	8690	1050
100.0	7640	7700	6560	
300.0		5160		

Table 3. Comparison of Calculated and Measured Pressures for Tunnel Complex.

Gage Position	Tunnel Complex Measured Peak Pressures (kPa)	Calculated Peak Pressures Using Autodyn		
		Autodyn-2D Non-Responding Wall Surfaces (kPa)	Autodyn-2D Responding Wall Surfaces (kPa)	Autodyn-3D Responding Wall Surfaces (kPa)
26	13103	24510	24880	15770
25	2898			8200
17	6750	7800	7220	6580
16	1660			5100
11		9870	6440	4200
10	1050	16500	13540	645

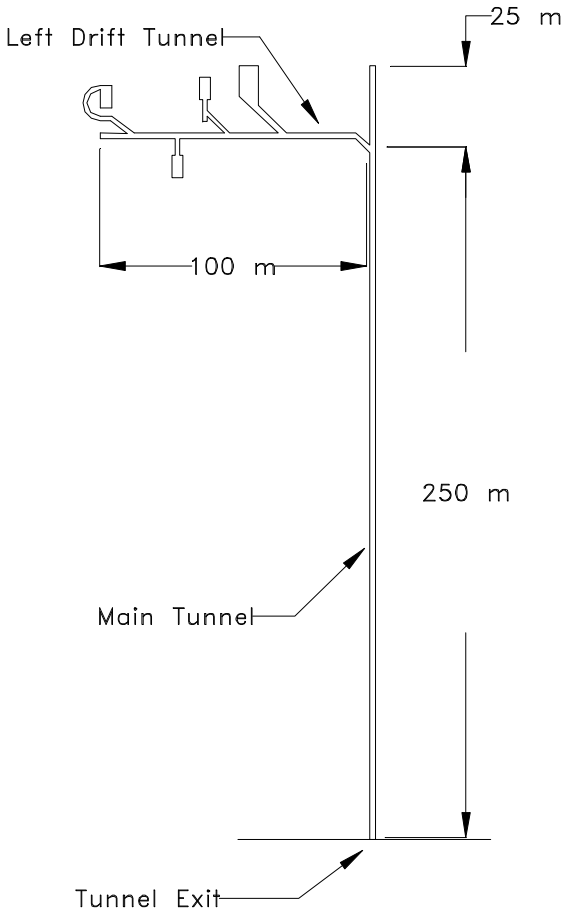

Figure 1. Layout of Underground Tunnel Complex.

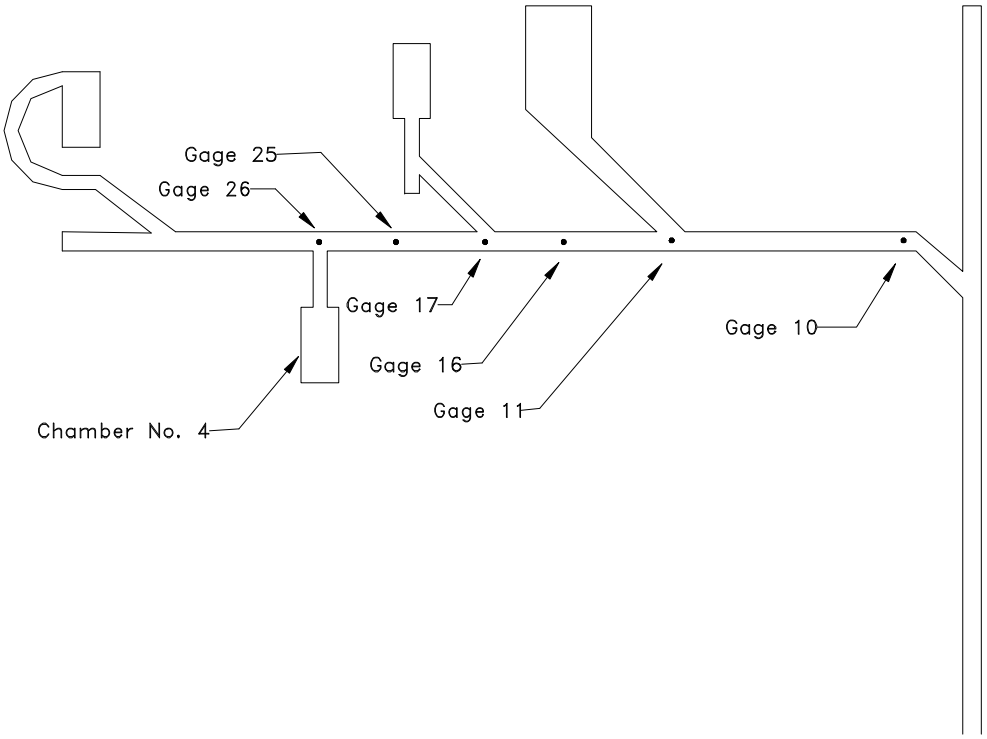

Figure 2. Locations of Pressure Gages in Left Drift Tunnel.

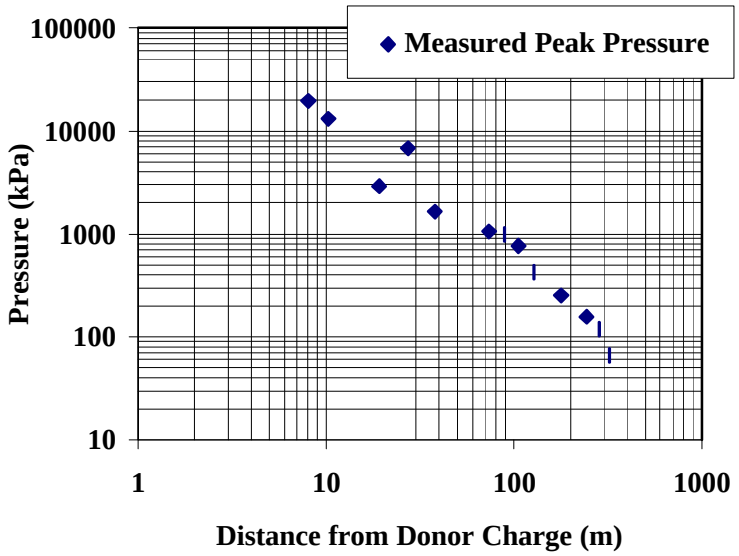

Figure 3. Measured Peak Side-on Pressures for Tunnel Test.

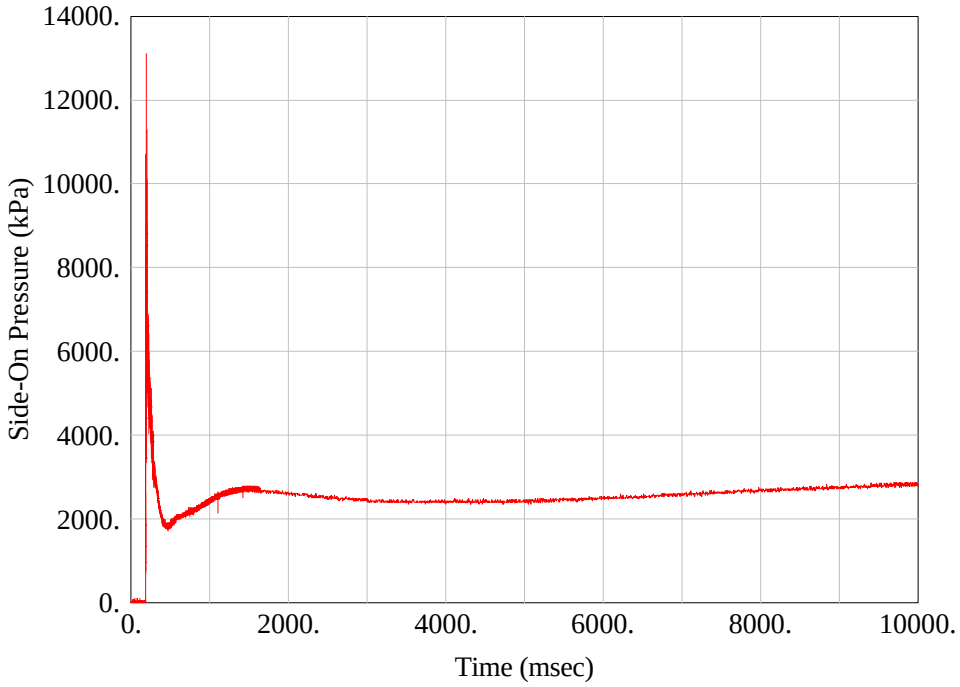

Figure 4. Pressure Time History at Gage 26, Left Drift in Front of Access Tunnel.

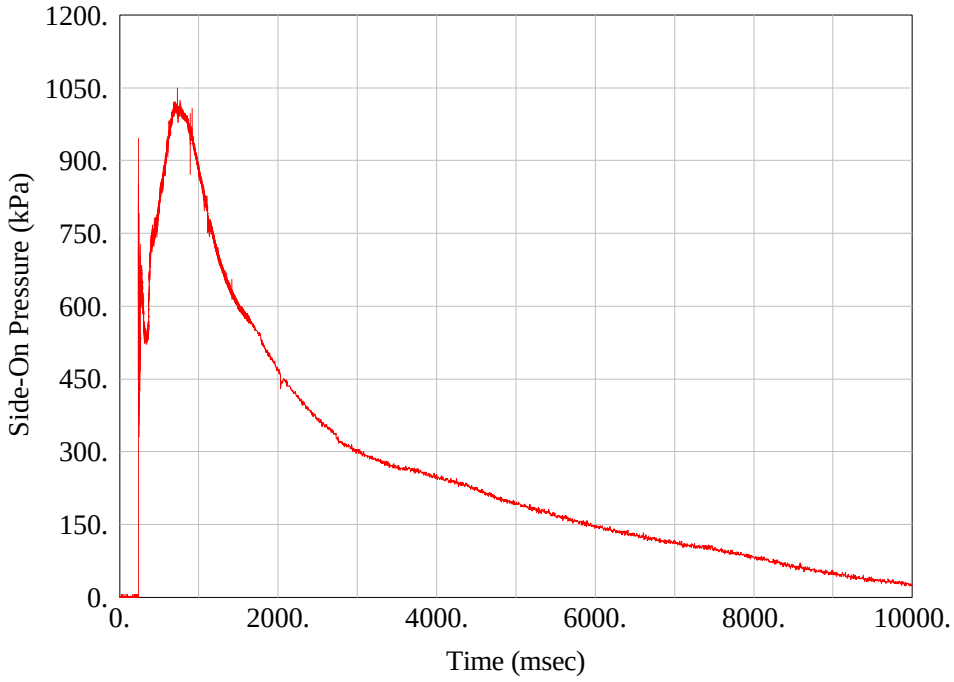

Figure 5. Pressure Time History at Gage 10, Junction of Left Drift and Main Tunnels.

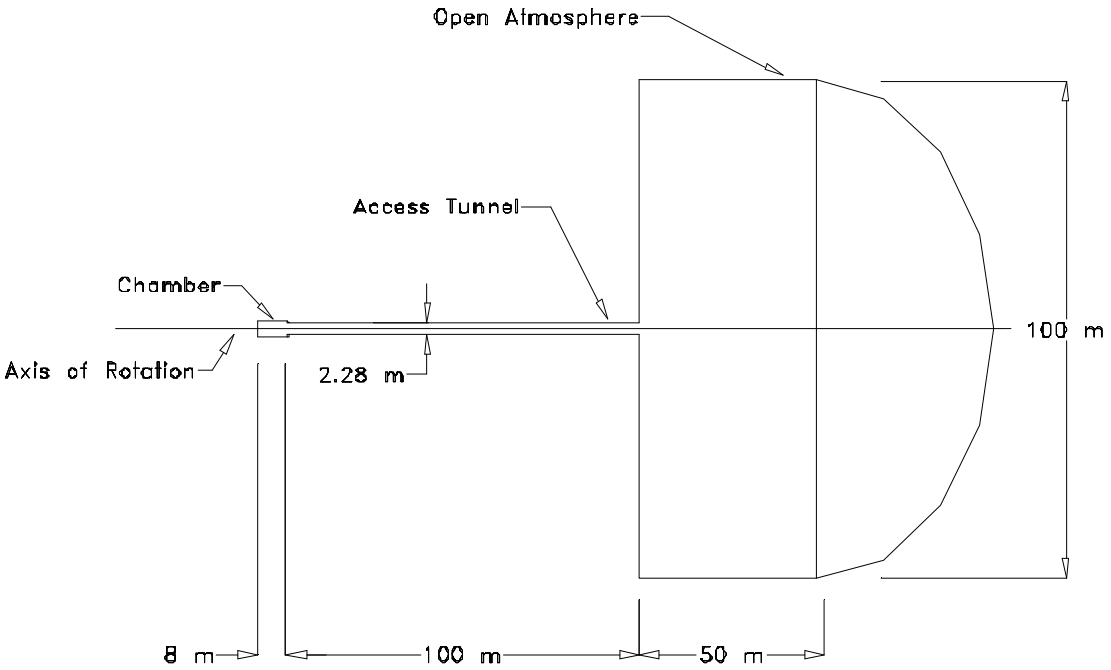

Figure 6. Typical Autodyn-2D Model of Straight Tunnels without Responding Media.

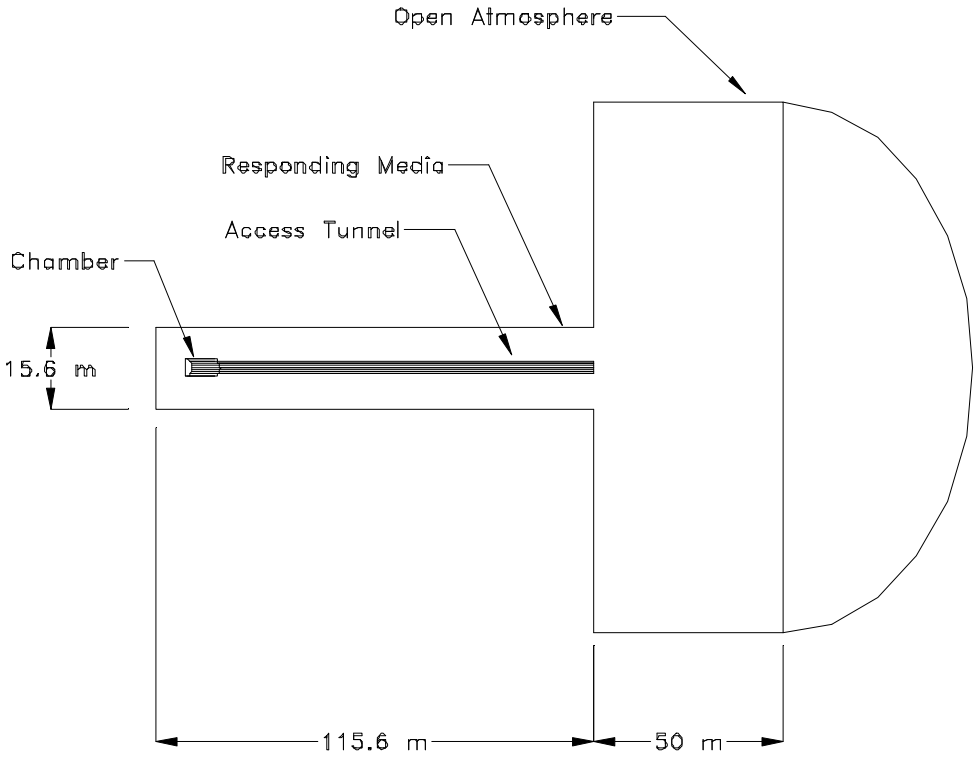

Figure 7. Typical Autodyn-2D Model of Straight Tunnels with Responding Media.

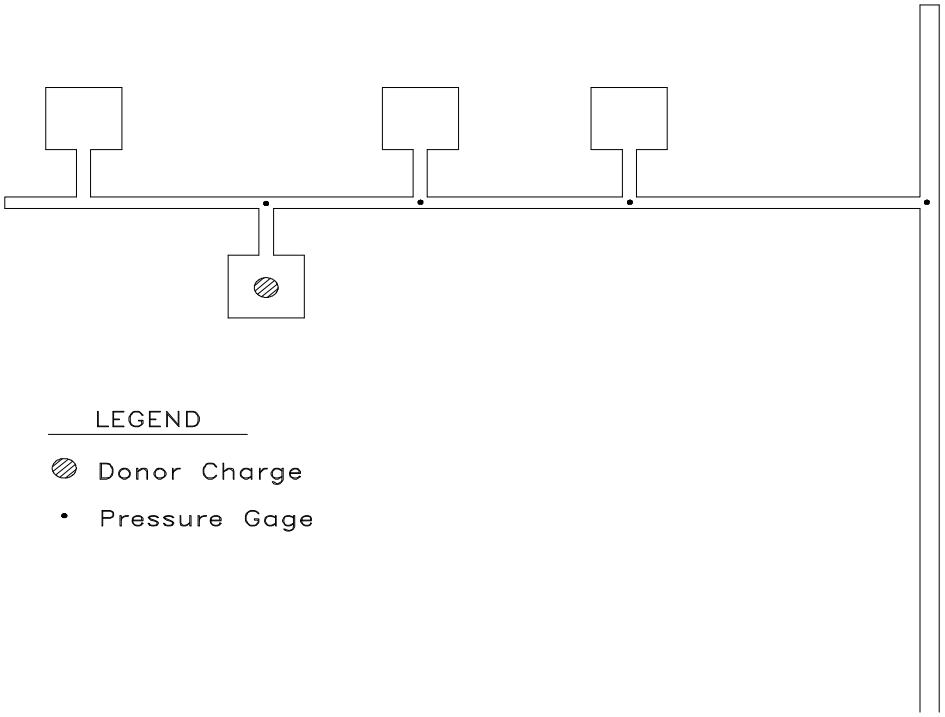

Figure 8. Typical Autodyn-2D Model of Tunnel Complex without Responding Media.

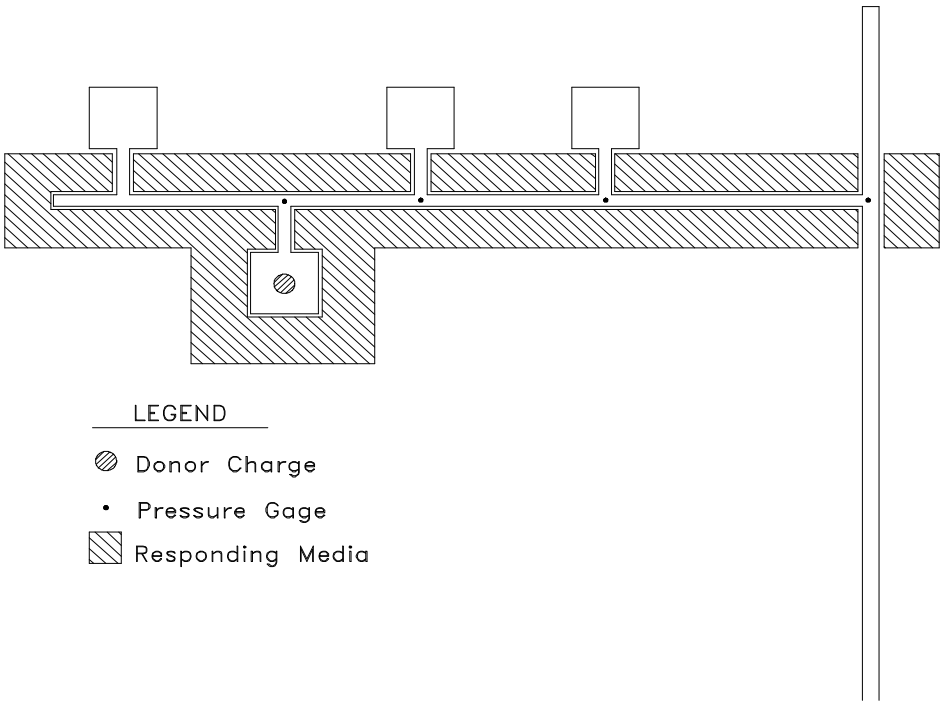

Figure 9. Typical Autodyn-2D Model of Tunnel Complex with Responding Media.

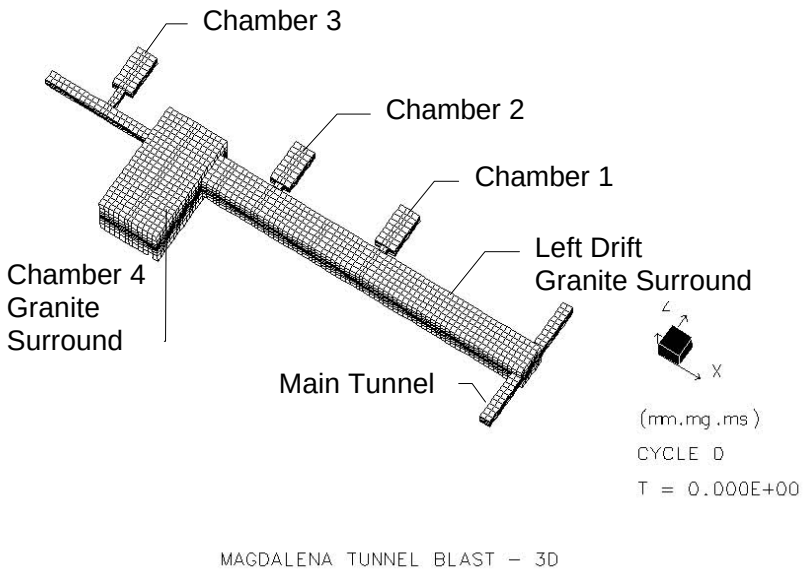

Figure 10. Autodyn-3D Model of Left Drift Tunnel and Test Chambers.

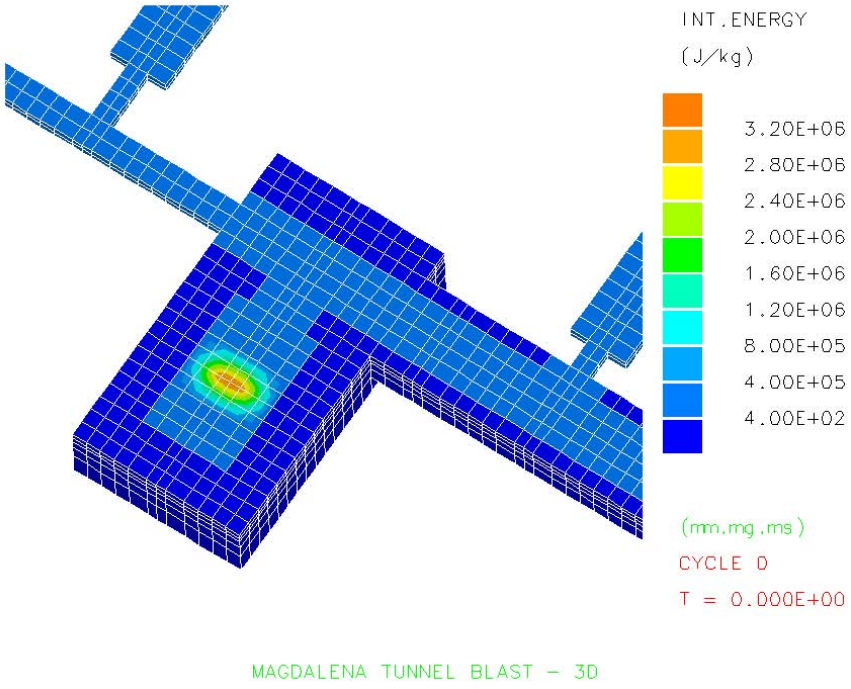

Figure 11. Detonation of Donor Charge inside Chamber No. 4.

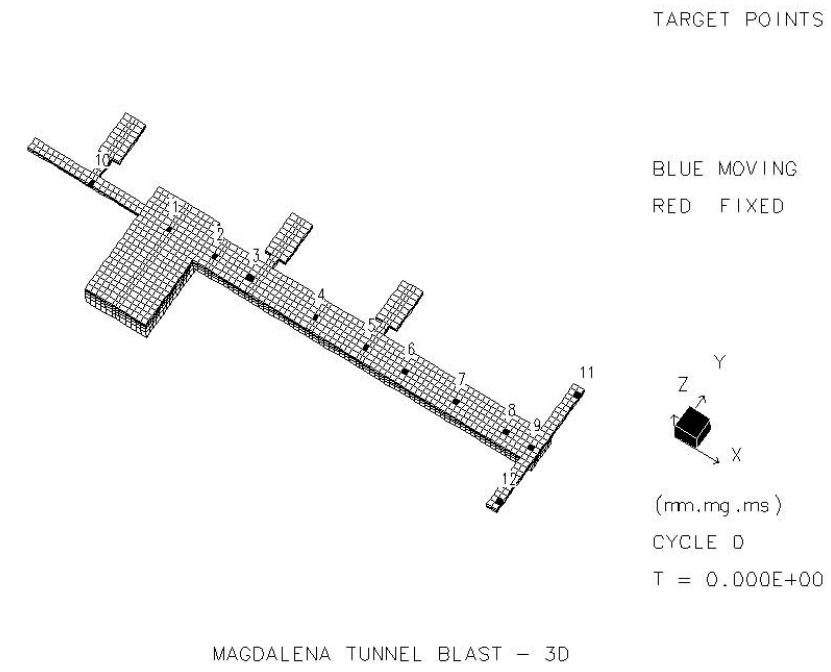

Figure 12. Target Locations for Calculating Pressure Time-Histories.

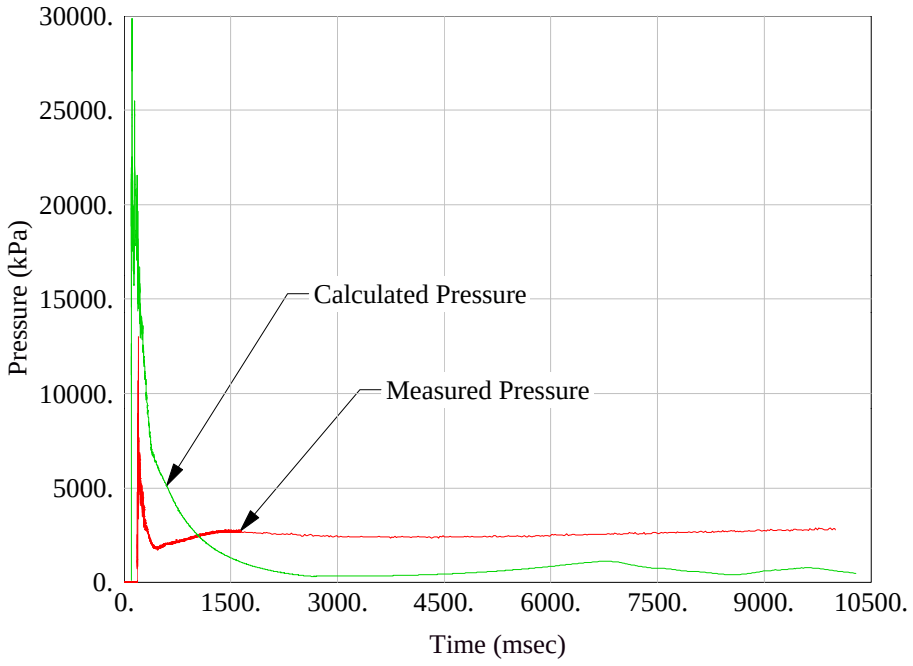

Figure 13. Calculated and Measured Pressure Time-Histories, Left Drift Tunnel in Front of Chamber No. 4 Access Tunnel.

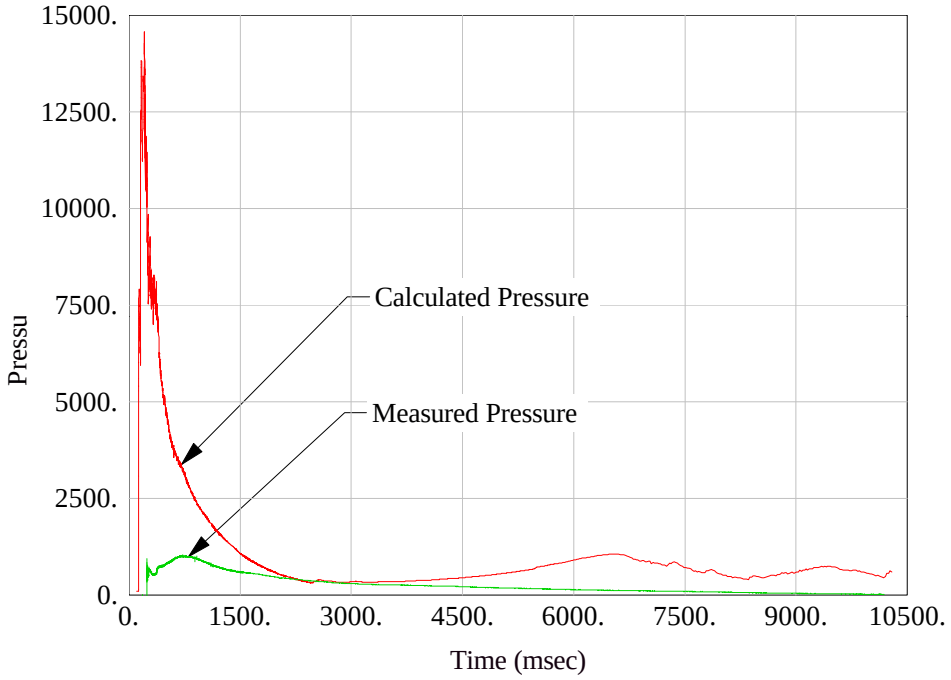

Figure 14. Calculated and Measured Pressure Time-Histories, Junction of Left Drift Tunnel and Main Tunnel.

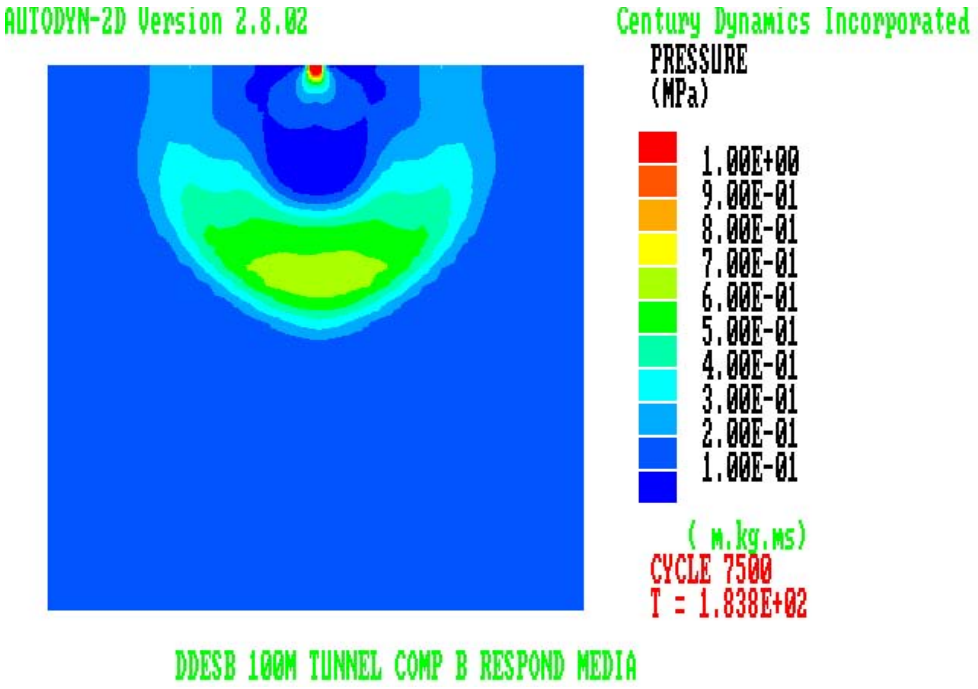

Figure 15a. Pressure Contour of Shock Wave Exiting Main Tunnel, t=183.8 msec.

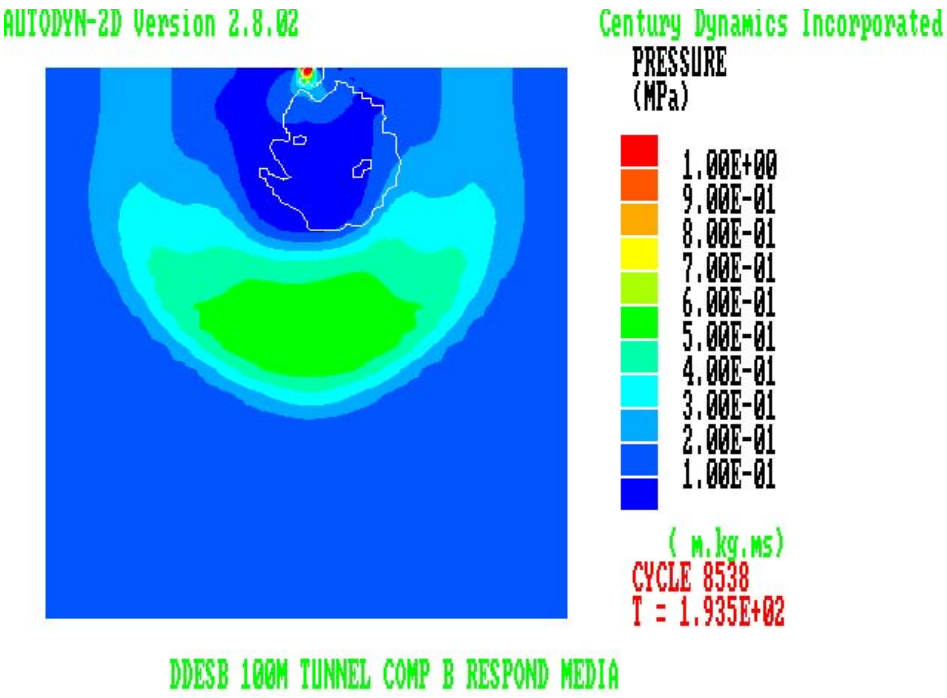

Figure 15b. Pressure Contour of Shock Wave Exiting Main Tunnel, t=193.5 msec.

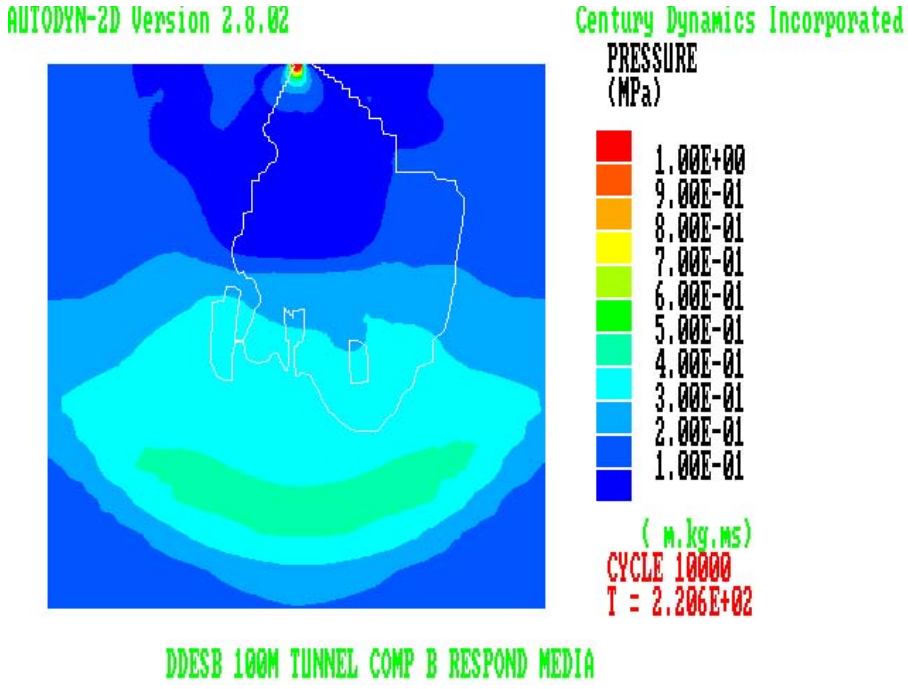

Figure 15c. Pressure Contour of Shock Wave Exiting Main Tunnel, t=220.6 msec.

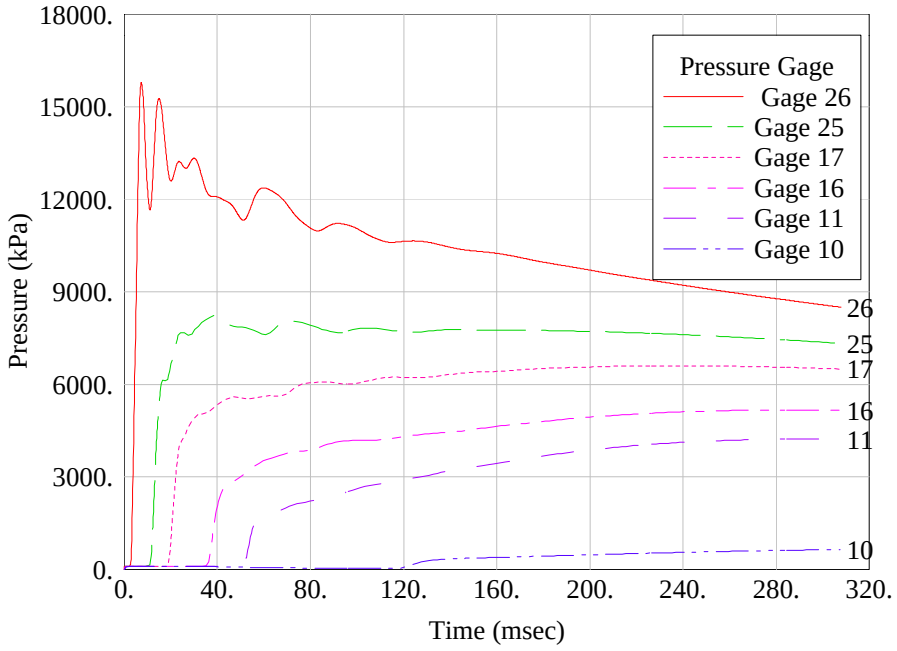

Figure 16. Calculated Pressure Time-Histories, Autodyn-3D Model.

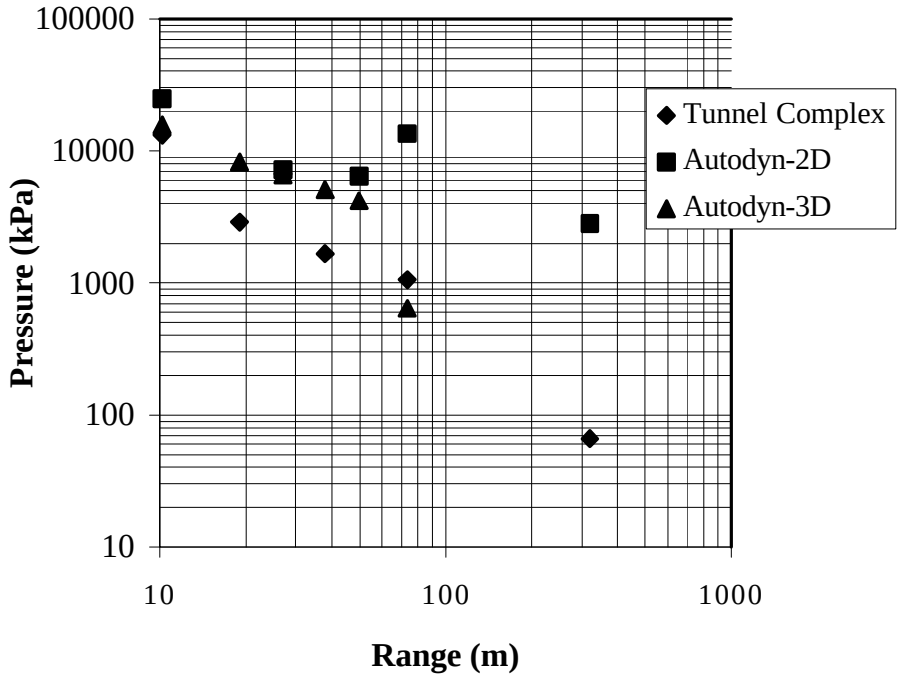

.

Figure 17. Comparison of Measured and Calculated Peak Pressures.